[Your Title Here]

by

[Your Name Here]

Department of [Your Department Here]
Duke University

Date: _____

Approved:

_____
[Your Supervisor Here], Supervisor

_____
[Department Committee Member #1]

_____
[Department Committee Member #2]

_____
[External Committee Member]

Dissertation submitted in partial fulfillment of the requirements for the degree of
Doctor of Philosophy in the Department of [Your Department Here]
in the Graduate School of Duke University
2014

Abstract

[Your Title Here]

by

[Your Name Here]

Department of [Your Department Here]
Duke University

Date: _____

Approved:

_____
[Your Supervisor Here], Supervisor

_____
[Department Committee Member #1]

_____
[Department Committee Member #2]

_____
[External Committee Member]

An abstract of a dissertation submitted in partial fulfillment of the requirements for the degree of Doctor of Philosophy in the Department of [Your Department Here] in the Graduate School of Duke University
2014

Abstract

Write your abstract here. You should not include references or mathematical notation.

If you want to dedicate your thesis to anyone do so here

Contents

List of Tables

List of Figures

List of Abbreviations and Symbols

Symbols

Put general notes about symbol usage in text here. Notice this text is double-spaced, as required.

$\mathbb{X}$	A blackboard bold X. Neat.
$\mathcal{X}$	A caligraphic X. Neat.
$\mathfrak{X}$	A fraktur X. Neat.
$\mathbf{X}$	A boldface X.
X	A sans-serif X. Bad notation.
X	A roman X.

Abbreviations

Long lines in the `symbollist` environment are single spaced, like in the other front matter tables.

AR	Aqua Regia, also known as hydrocloric acid plus a splash of nitric acid.
SHORT	Notice the change in alignment caused by the label width between this list and the one above. Also notice that this multiline description is properly spaced.
OMFGTXTMSG4ME	Abbreviations/Symbols in the item are limited to about a quarter of the textwidth, so don't pack too much in there. You'll bust the margins and it looks really bad.

Acknowledgements

Thank anyone you like here. It's good practice to thank every granting agency that's given you money since you've been ABD, any other school you visited during your research, and any professional society that's funded your travel.

[75mm] Nulla facilisi. In vel sem. Morbi id urna in diam dignissim feugiat. Proin molestie tortor eu velit. Aliquam erat volutpat. Nullam ultrices, diam tempus vulputate egestas, eros pede varius leo. Quoteauthor Lastname

1

The title of chapter one

- radiotherapia oggi (vs surgery and chemio) - serve fonte

- serve fonte, ho usato katia parodi

Results of radiotherapy are improved when a high dose of radiation with high biological effectiveness is delivered to the tumour with the least possible dose to the surrounding tissues, especially in the case of critical organs **?**. In order to increase the conformity of the dose delivered to the tumour, diverse technologies have been considered and used. Traditional forms of radiotherapy, X-ray tubes (energy $\sim$ 100 keV) or radioactive isotopes have been replaced by linear accelerators delivering $\sim$ 10 MeV from different directions (e.g. Intensity Modulated Radio Therapy), and provide treatment with photons and electrons. Though being widely used as a standard in radiation therapy, the effectiveness of conventional electromagnetic radiation is limited by the intrinsic characteristics of interaction with matter. In particular two aspects disfavours in principle the usability of electromagnetic radiation with respect to ion for tumour targeting: the depth dose profile, which does not allow for an optimal dose deposition to the tumour sparing vital organs and the inferior biological

FIGURE 1.1: Schematic view of depth-dose distributions of photons and ions. (a) photon field, (b) spread-out ion beam, (c) depthdose profiles along the central beam axis **?**.

effectiveness, which is the limiting factor in case of radio resistant tumours. Heavier charged particles, like protons and ions (He-Ca) have the potentiality to overcome the limits of conventional therapy With respect to this, the scientific community is directing his attention towards possible improvements of ion beam therapy **?**.

- qui citare entervision website

The work outlined in these pages have been sponsored by The European training network in digital medical imaging for radiotherapy (ENTERVISION) at the European Center of Nuclear Research (CERN). ENTERVISION was established in February 2011 in response to the critical need for reinforcing research in online 3D digital imaging and the training of professionals in order to deliver some of the key elements and building blocks for realizing the vision for early detection and more precise treatment of tumours.

1.1 Hadrontherapy

1.1.1 Ion beam therapy

The first proposition of ion beam therapy was presented in 1946 by R. Wilson **?**. The original idea was exploit the physical properties of ion interaction in matter to improve the precision in radiotherapy treatments. Making use of the so called Bragg peak, that is using the fact that protons and ions in general deposit a maximum of energy at the end of their trajectory, the treatment could save the surrounding tissue from radiation overdose.

The dose deposited by photons, considered as the gold standard for tumour treatment, is maximum close to the beginning of the trajectory in the body and is characterized by an exponential decrease. As a consequence an undesired radiation dose

is delivered to healthy tissues around the targeted tumour.

The recent therapeutic interest of ions in the field of radiotherapy relies mainly on their high relative biological effectiveness. LET (linear energy transfer) has long been viewed as the main parameter to discern the biological effect of different kinds of radiation. It is a measure for the energy deposited by a charged particle traveling through matter. LET is closely related to stopping power and is not a constant value, since it changes along the particle's path (es 10 kEV/um for gamma, 100 kev/um for protons, 1000 kev/um for ions). When considering ions of different atomic number LET becomes a limited parameter to evaluate the biological effect. In this sense the relative biological effectiveness (RBE) is considered the most accurate quantity, since it is defined as the biological effect of one type of ionizing radiation relative to another, given the same amount of absorbed energy. As the charge of the incident ions increases, so does the probability of severe DNA damage. An elevate RBE in the Bragg peak region has clearly been demonstrated for ions heavier than Helium **?**. As a consequence they prove to be more effective for targeting radio resistant or inoperable tumours.

1.1.2 Beam delivery

Ion beams are delivered by either cyclotrons or synchrotrons. In the first case the beam has a fixed energy which is tuned by means of degraders in order to deliver the correct dose profile. In the case of synchrotron the beam is delivered in spills and the energy is varied between spills. In the case of Carbon only synchrotrons can be used. To deliver the dose to the planned target volume (PTV) different energies are superimposed in order to obtain the so-called spread-out Bragg peak (SOBP). The beam is usually delivered in a passive beam shaping setup or a scanning system.

Different sources of error can worsen the dose delivery profile, such as patient mis positioning and evolution of the tumour/morphology of the patient. In addition the

complex physics of ion interaction leads to imprecision in the treatment plannings, due to fragmentation of the incident beam and range uncertainties.

Usually treatment planning systems cope with these problems by irradiating a volume larger than the tumour itself, called planning target volume (PTV) which contains the CTV. Complex compensating systems, including x-ray imaging techniques and patient positioning systems, allow to reduce errors in the dose profiles delivered. Treatment plannings of ion therapy relies for example on accurate values of particle range in tissue obtained from Hounsfield unit of computed tomograms, leading to uncertainties of $1-3\%$ in range calculations **?**. The dose delivered by a ion beam system is much more sensitive to these deviations than the one delivered by a photon beam. Due to the high biological effectiveness of ion beams wrong ranges could lead to dramatic under dosage to the tumour or over dosage to organ at risk surrounding. As a consequence a three-dimensional non invasive imaging technique for ion beam therapy monitoring is required. Since ions, unlike photons, are stopped completely in the patient volume, technology like portal imaging are not suitable. The attention of the community is thus focused on positron emission tomography (PET), which relies on the peculiar characteristics of $\beta+$ decay.

1.1.3 Monitoring of the beam

Several attempts have already been undertaken to systematically assess the benefit of the PET method for beam monitoring, the principal one being the set up installed at the experimental carbon ion therapy unit at the Gesellschaft fur Schwerionenfroschung Darmstadt (GSI) **?**. Two alternatives can be considered: the use of positron radioactive ions as projectiles for dose delivery or the detection of $\beta+$ activity given bi nuclei fragmentation. As an example of the first approach it is interesting to consider the effort made at the Heavy Ion Accelerator in Chiba (Japan), where radioactive beams of ^{11}C $-^{10}C$ ions deliver an activity of $10^3 - 10^5$ $BqGy^{-1}cm^{-3}$

within the irradiated volume. Due to the low production rate of secondary radioactive ions, this approach has been only partially successful. Another possibility is to make use of the $\beta+$ activation given by the fragmentation of stable ions interacting with the tissue. The radioactivity is a direct product of the irradiation and, although the activity density is rather low (around 600 $BqGy^{-1}cm^{-3}$ for protons), this method provides a rather cheaper and feasible solution **?**. The activity slides very fast under a reasonable threshold for detectability and the most effective solution is an in-beam scanner. In-beam PET is currently the main method implemented clinically for in situ monitoring of charged hadron radiotherapy**?**.

1.2 Positron Emission Tomography

1.2.1 Principles

Positron Emission Tomography (PET) has been introduced as a nuclear medicine imaging technique which measures the distribution of a positron-emitting radionuclide (tracer), which is injected into the body on a biologically active molecule. In the case of in-beam PET the activity is present in the body of the patient due to the activation induced by proton interaction. After the injection, or during the dose delivery, the subject of a PET study is placed within the field of view (FOV) of a number of detectors capable of registering incident gamma rays. The radionuclide in the radio tracer decays and the resulting positrons subsequently annihilate with electrons after travelling a short distance ($\sim$ 1 mm) within the body. In the case of in-beam PET activation of the tissues guarantees the detectability. Each annihilation produces two 511 keV photons travelling in opposite directions and these photons may be detected by the detectors surrounding the subject. The detector electronics are linked so that two detection events unambiguously occurring within a certain time window may be called coincident and thus be determined to have come from the same annihilation. These "coincidence events" can be stored in arrays

corresponding to projections through the patient and reconstructed using standard tomographic techniques. The resulting images show the tracer distribution throughout the body of the subject. The scheme of a PET scanner is shown in figure **??**. Positron emission tomography relies on the β^+ decay of a radionuclide.

The nucleus of the radionuclide can convert a proton into a neutron

$$p \rightarrow n + e^+ + \nu_e$$

As positrons travel through human tissue, they give up their kinetic energy principally by Coulomb interactions with electrons. As the rest mass of the positron is the same as that of the electron, the positrons may undergo large deviations in direction with each Coulomb interaction, and they follow a tortuous path through the tissue as they give up their kinetic energy.

When the positrons reach thermal energies, they start to interact with electrons either by annihilation, which produces two 511 keV anti-parallel photons, or by the formation of a hydrogen-like orbiting couple called positronium. In its ground-state, positronium has two forms: ortho-positronium, where the spins of the electron and positron are parallel, and para-positronium, where the spins are anti-parallel. Para-positronium again decays by self-annihilation, generating two anti-parallel 511 keV photons. Ortho-positronium self-annihilates by the emission of three photons. Both forms are susceptible to the pick-off process, where the positron annihilates with another electron. Free annihilation and the pick-off process are responsible for over 80% of the decay events.

1.2.2 Image reconstruction

1.2.3 Sources of noise and sensitivity

In a PET scanner, each detector generates a timed pulse when it registers an incident photon. These pulses are then combined in coincidence circuitry, and if the pulses

fall within a short time-window, they are deemed to be coincident (see figure). A coincidence event is assigned to a line of response (LOR) joining the two relevant detectors. In this way, positional information is gained from the detected radiation without the need of a physical collimator. This is known as electronic collimation. When a physical collimator is used, directional information is gained by preventing photons which are not normal or nearly normal to the collimator face from falling on the detector. In electronic collimation, these photons may be detected and used as signal. Coincidence events in PET fall into four categories: true, scattered, random and multiple, as shown in figure .

True coincidences occur when both photons from an annihilation event are detected by detectors in coincidence, neither photon undergoes any form of interaction prior to detection, and no other event is detected within the coincidence time-window.

A scattered coincidence is one in which at least one of the detected photons has undergone at least one Compton scattering event prior to detection. Since the direction of the photon is changed during the Compton scattering process, it is highly likely that the resulting coincidence event will be assigned to a wrong LOR. Scattered coincidences add background to the true coincidence distribution which changes slowly with position, decreasing contrast and causing the isotope concentrations to be overestimated. They also add statistical noise to the signal. The number of scattered events detected depends on the volume and attenuation characteristics of the object being imaged, and on the geometry of the PET scanner.

Random coincidences occur when two photons not arising from the same annihilation event are incident on the detectors within the coincidence time window of the system. The number of random coincidences in a given LOR is closely linked to the rate of single events measured by the detectors joined by that LOR and the rate of random coincidences increase roughly with the square of the activity in the FOV. As with scattered events, the number of random coincidences detected also depends on

the volume and attenuation characteristics of the object being imaged, and on the geometry of the scanner. The distribution of random coincidences is fairly uniform across the FOV, and will cause isotope concentrations to be overestimated if not corrected for. Random coincidences also add statistical noise to the data.

1.2.4 TOFPET

It has been shown that in-beam PET could not provide definitive information to the oncologist when medium to large tumors are involved**?**. This is due to the operative parameters of scanners available on the market, with relatively slow scintillators and tomographs covering small solid angles. A decisive improvement could be given by time-of-flight PET (TOF-PET).

Recent developments in scintillator technology and read out electronics allow to build detectors able to detect the time difference between the moment of detection of the opposed gamma rays in coincidence.

If we define a LOR between two detectors A and B, the distance between the center of the LOR and the annihilation point is given by

$x = (tbta)c/2$

where c is the speed of light. Thus the spatial resolution is proportional to the coincidence time resolution (CTR) of the system. Scanners available on the market today could deliver a 600 picoseconds time resolution, that translates to a positional uncertainties of 9 cm (FWHM) on the LOR. The quality of the tomographic image largely benefits from the timing information of a TOFPET scanner, since it reduces considerably the contribution of Compton scattered photons and from photons from outside the field-of-view (FOV). As a consequence the background from scattered and random coincidence is largely suppressed. The signal to noise ration (SNR) is thus dramatically improved. In the case of in-beam PET this is relevant, since it has been shown (Fiedler et al 2007) that during particle irradiation an considerable

amount of activity is transported outside the FOV by metabolic processes. Moreover a high backround signal is typical of carbon ion beams (Pawelke 1997)

A useful and pratical estimation of the gain in signal to noise can be formalized as follows

$G = \frac{SNR_{TOF}}{SNR_{non_TOF}} = \sqrt{\frac{2 \cdot D}{c \cdot CTR}}$

where D is the diameter of the volume under examination, c is the speed of light and CTR is the coincidence time resolution. Thus a CTR of 100 ps FWHM translates into a 1.5cm resolution on the position and a SNR gain of 5 (corresponing to a sensitivity gain of about a factor 25) compared to non TOF systems.

1.3 Outline of the thesis

The work presented in this thesis is devoted to the improvement of the operational parameters of TOFPET used in hadrontherapy, with particular respect to fast timing in particle detectors.

1.4 From high energy physics to medical applications

The present work was hosted by CERN, the European Organisation of Nuclear Research, based in Geneva, Switzerland. CERN was established by a formal act in Paris, on 1st of July 1953, as an organisation that shall provide for collaboration among European States in nuclear research of a pure scientific and fundamental character, and in research essentially related thereto -. Thourought its history, CERN provided experimetnal and theoretical tools to study and understand the fundamental forces governing our universe, in a continous effort to improve our understanding of elementary physics.

The Large Hadron Collider (LHC), the last effort of scientific community around CERN facility, is the most powerful particle accelerator ever built, expected to ac-

celerate proton beams to an energy of up to 7 TeV maintaining a luminosity of 1034 cm-2s-1. The work here presented has been hosted by the CERN section responsible for the development and construciont of the electromagnetic calorimeter (ECAL) of the CMS (Compact Muon Solenoid) experiment. CMS is a multipurpose detectors used at LHC devoted to the identification and discoveries of new particles and evidence of physics beyond the standard model. It is composed by a 4 T solenoid magnet and several concentric subdetectors that include a tracker, an electromagnetic and a hadronic calorimeter and various layers of muon detectors. The ECAL detector was build with the fundamental contribution of the collaboration hosting this thesis: the Crystal Clear Collaboration. It was founded in 1990 as an international academic network of laboratories and industrial partners for the development of scintillating crystal detectors as well as their applications. It comprises experts in crystallography and solid state physics as well as in radiation detection and instrumentation. Its first goal was the development of a radiation-hard crystal for the ECAL detector, leading to the development of PbWO4 (PWO) as the material selected for CMS calorimeter. More recently the group has been focusing on the study of new materials for hadronic and electromagnetic calorimeters for future particle accelerators. In parallel, the collaboration engaged in a effort of technology transfer to other domains exploiting the expertise developed in scintillating detectors. It is quite natural to focus the attention to medical physics, with particular respect to nuclear medicine. As shown in picture () the requirements for detectors used in medical physics and detectors for high energy experiments are similar.

1.4.1 Study of time profiles

- outline vero e proprio - panorama pubblicazioni - obiettivi - strumenti (simulazioni e setups) - misure

$x = 1/\alpha$

$$\zeta = \frac{1039}{\pi}$$

Fig. **??**.

[75mm] This is some random quote to start off the chapter. Firstname lastname

2

Scintillating detectors

2.1 Introduction to particle detectors

In the field of medical applications, the energies of the gamma photons to be detected are usually of the order of hundreds of keV. In the case of PET scanners the energy of the two back to back photons is 511 keV. A simple approach to estimate the parameters of the incoming radiation is to make use of a fluorescent sample coupled to a photodetector. A standard set up would include a heavy scintillator crystal which converts the incoming radiation into visible photons. The following steps of the detection process involve transportation to the entrance window of the photodetector, conversion of the photons into an electric signal and subsequent manipulation of the signal by readout electronics.

2.2 Interaction of radiation with matter

In this work we are mainly concerned with the interaction of gamma radiation with matter, thus focusing our attention to the three existing mechanisms: photo electric interaction, Compton interaction and pair production. A brief description of

Rayleigh scattering will be given, as a non-ionizing type of scattering. Moreover electrons produced by ionizing interactions can polarize the medium, giving origin to the Cerenkov effect and producing visible photons, which can be of foremost importance in the case of timing application.

2.2.1 Photoelectric effect

In the case of the photoelectric effect an electron from an atom is freed upon absorption of the incoming photon:

$$\gamma + atom \rightarrow e^{-} + atom \tag{2.1}$$

Due to conservation of momentum and energy this phenomenon does not occur with free electrons. The gamma energy trasnferred to the electron equals the binding energy of the electron itself minus its resulting kinetic energy E_{e-}

$$E_{e^-} = E_{\gamma} - E_b \tag{2.2}$$

The photoelectric effect is predominant at low energies ($E <= 100keV$) and favours tightly bound K-shell electrons. An approximation of the photo electric cross section is given by

$$\sigma_{pe} \frac{Zn}{E_{\gamma} 3.5} \tag{2.3}$$

The vacancy created can be filled through capture of bound or free electrons, eventually generating characteristics X-rays.

2.2.2 Compton scattering

Compton scattering is the inelastic scattering of the incoming photon with a weakly bound electron in the material.

$$\gamma + atom \rightarrow (\gamma') + e^{-} + atom* \tag{2.4}$$

Contrary to the photoelectric effect, this only concerns quasi-free electrons of the material. The photon trasnfers part of its energy to the electron, which is freed from its shell. Applying conservation of energy and momentum it is possible to derive the energy of the scattered gamma as well as the direction and energy of free electron.

$$E_{\gamma'} = \frac{E_\gamma}{1 + \frac{E_\gamma}{m_e c^2}(1 - cos\theta)} \tag{2.5}$$

The angular distribution can be described by the Klein-Nishina formula. It is evident from the plot that forward scattering direction are favoured as the incoming photon energy increases

$$\frac{d\sigma_{cpt}}{d\omega} = Z \cdot \frac{e^2}{4\pi\epsilon_0 m_e c^2} \cdot \frac{1}{2} \cdot \frac{E'_\gamma}{E_\gamma} 1 - \frac{E'_\gamma}{E_\gamma} \cdot sin^2\theta + \left[\frac{E'_\gamma}{E_\gamma}^2\right] \tag{2.6}$$

The total cross section can be computed by integrating the differential cross section over the angle.

2.2.3 Pair production

If the energy of the gamma exceeds $2m_e c^2 = 1.02MeV$, the impinging photons can also be converted into an electron-positron pair. The cross-section of the pair production is given at low energies (thus low screening) by

$$\sigma_{pair} = 4\alpha r_e^2 Z^2 \left(\frac{7}{9} ln2 \frac{E}{m_e c^2} - \frac{109}{54}\right) \tag{2.7}$$

The cross section is very low compared to that of photoelectric and Compton effect until the energy of the gamma approaches several electron Volts. Thus for the energies involved in medical applications pair production can be neglected.

2.2.4 Rayleigh scattering

2.3 The scintillation mechanism

As a general idea the scintillation process can be considered as the conversion of the energy of an incident gamma quantum or particle into a certain number of low energy photons**?**. In a way it can be therefore defined as a wavelentgh shifting process**?**.

After a ionization event, generated by the mechanisms presented above in the case of a gamma interaction, the scintillator relaxes towards a new equilibrium. This process is characterized by a multitude of sub processes, that can be depicted by band diagrams as the one in picture. As long as the energy of the particles is high enough, it is transferred to secondary particles of low energy, creating an electromagnetic cascade. A crystal though is an ordered ensemble of atoms, so the electrons in the keV range start to couple with electrons and atoms of the lattice. As a result of their interaction with electronic states of the material, couples of electrons and relative vacancies are created. The electron hole pairs migrate in the lattice above and below the ionization threshold until they are trapped by a defect or recombine on a luminescent center. Alternatively they cool down by coupling to the lattice vibrations until they reach the top of the valence band (hole) or the bottom of the conduction band (electron). They can also form loosely bound structures called exciton, with en energy slightly smaller than the bandgap energy. The scintillator itself must contain luminescent centers, either intrinsic or extrinsic (doping ions). These molecular systems in the lattice present characteristic transitions between excited states. The scintillation process can therefore be represented as the sequence of the following stages**?**:

- Absorption of ionizing radiation and creation of primary e-h pairs
- Relaxation of primary e-h pairs with production of secondary e-h pairs, plas-

mons, photons, etc.

- Thermalization of low energy e-h pairs down to the band gap energy E_g
- Energy transfer form the e-h pairs to the luminescence centers
- Emission of scintillation photons

2.3.1 Creation of electron hole pairs

To analyze more in depth the mechanisms of the scintillation, we can consider an intermediate energy gamma ray ($500keV$) interacting with the scintillator material. In this case the photoelectric effect is dominant. Thus it will produce a hole in a inner shell (usually K shell) and a free or quasifree electron.

$$A + h \ni \rightarrow A^+ + e \tag{2.8}$$

The energy of the primary electron will be $h \ni -E_k$ where E_k is the K level energy.

The relaxation then happens differently for electrons and holes.

The ionized atom (A^+) can relax either radiatively, thus emitting a photon, or nonradiatively, generating a secondary electron. This is know as the Auger effect. Thereafter a cascade of both radiative and nonradiative processes take place. The Auger electron and the primary electron begin a proces of electron-electron scattering or phonon emission. In the case of a radiative emission, the soft x-ray photon emitted may be absorbed producing a new deep hole and free electron.

The electron on the other hand will ionize an atom

$$A + e \rightarrow A^+ + 2e \tag{2.9}$$

The two undistiguishable electrons will undergo a number of other ionization processes, resulting in an avalanche of secondary electrons and holes. At some point the secondary products of these processes are not able to ionize the medium anymore. A

fast electron can in principle interact also with valence electrons of the medium, producing collective oscillations known as plasmons. Plasmons behave as quasiparticles, with an energy of $10eV$ and can decay into e-h pairs.

This ensemble of avalanche processes continues until the generated secondaries are not able to create further ionization. At this point electrons and holes start to interact with the vibrations of the lattice in a stage called thermalization, via different mechanisms of electron-phonon interaction. As a consequence, at the end of this chain of de-excitation processes, low energy electronic excitations are present: electrons in the conduction band, holes in the valence band, valence excitons, core excitons.

2.3.2 Intrinsic luminescence

Electron and holes have several ways to recombine after thermalization and give rise to scintillation photons. The simplest emission process is direct recombination

$$e + h \rightarrow h \ni \tag{2.10}$$

Recombination can more effectively take place when the energy of the electron and hole has decreased, so that they form a loosely bound structure called exciton. However the various impurities and lattice defects play a very important role in the scintillation process. Thermalized carriers can be bound in some places of the lattice where atom or defects are localized. For example many ionic crystals shows phenomena of localization of the valence hole in the lattice, known as self-trapping. This structure appears when a thermalized hole localizes an anion, polarizing the environment. As a result the hole can be shared between two neighbouring ions forming a V_k center, and the hole is defined as self-trapped hole. For high energy excitation direct creation of valence exciton is unlikely, so V_k centers usually capture free electrons. From subsequent de excitation they can emit photons, thus giving

rise to the excitonic luminescence.

$$e + h \rightarrow ex \rightarrow h \ni \tag{2.11}$$

2.3.3 Core to valence transitions

If the core bands of the scintillator lie below the Ager threshold, the most favoured transitions involve holes in the valence band and electron in the conduction band. Some systems though present the so-called cross luminescence. This phenomenon implies a direct core to valence transition, due to the fact that holes in uppermost core bands can not deexcite non radiatively**?**.

A notable example of core to valence transition is BaF_2. In this system a Ba^{2+} $5p$ core hole is above the Auger threshold and hence Auger effect does not occur. They can recombine directly with electrons from the valence band, in most of the cases radiatively. This leads to a very fast luminescence given by recombination of the core hole, while the primary electron de excitation is more complex thus leading to a slower component.

2.3.4 Extrinsic luminescence

The scintillator samples used in this work are extrinsic, that is doped with activation centers that can enhance the intrinsic scintillation properties presented above by favouring direct recombiantion. Rare earth ions doping, for example, is largely used in scintillator technology because of the parity and spin-allowed transition $4fn - 15d \rightarrow 4fn$. Extrinsic scintillators usually present different luminscent mechanisms driven by activated sites**?**:

- $e + h + A \rightarrow ex + A \rightarrow A* \rightarrow A + h \ni$
- $e + h + A \rightarrow A^{1+} + e \rightarrow A* \rightarrow A + h \ni$
- $e + h + A \rightarrow (A^{1-}) * + h \rightarrow A + h \ni$

- $A \rightarrow A* \rightarrow A + h \ni$

In the first case the insertion of dopants is able to sufficiently quench the exciton luminescence so that excitation of radiative centers results form a transfer from excited matrix states. A copeting process is the direct capture of free thermalized carriers by luminescent center, in the case of electrons or holes. In heavy doped or self-activated crystals (CeF_3) direct excitation by ionizing radiation is possible.

2.4 Quenching phenomena

2.4.1 Light yield

One of the feature commonly required of a scintillator is to be have a high light yield, that is to be an efficient converter of radiation to visible light. In this case the relative light output of the scintillator, L_R, can be considered the significant quantity. It is defined as the number of emitted photons per unit of absorbed energy**?**

$$L_R = \frac{N_{ph}}{E_\gamma} \tag{2.12}$$

The number of produced e-h pairs N_{eh} depends on the average energy needed for the creation of a low energy e-h pair, χ_{eh}. This value depends on the type of lattice and band gap of the material, with a numericl coefficient β

$$\chi_{eh} = \beta \cdot \ E_g \tag{2.13}$$

If α is the average number of scintillation photons produced by a single e-h pair, the light output is

$$L_r = \frac{\alpha \cdot N_{eh}}{E_\gamma} = \frac{\alpha}{\chi_{eh}} = \frac{\alpha}{\beta \cdot_g} \tag{2.14}$$

The coefficient α depends on the transport efficiency of the e-h pairs to the luminescence center and the conversion efficiency of the center itself.

2.4.2 Optical properties and light transport

Moreover it is clear that the emission band of a scintillator should lie in the spectral range of the optical transmission of the crystal.

2.4.3 Energy resolution and nonproportionality

In the case of gamma spectroscopy ut is necessary to discriminate quanta with different energy. For scintillation detector this fundamental property is characterized by the energy resolution R, defined as Δ/E (in %) where ΔE is the full width at half maximum (FWHM) at pulse height E. It depends on the characteristics of the scintillator, i.e. materials, size and defects as well as the coupling with the photo detector and the parameters of the photo detectors itself. Statistical fluctuations at any step of the detector chain, from dynode multiplication from photocathode efificency in the case of a PMT can worsen the resolution at the peak. Thus energy resolution can be defined as**?**

$$R^2 = R_S^2 + R_{PM}^2 = R_S^2 + \frac{\delta}{E_\gamma} \tag{2.15}$$

where R_S and R_{PM} are, respectively, the scintillator and photomultiplier contributions and δ includes photo electron statistics. It is possible to further decompose the scintillator resolution R_S to take into account the factors depending on the type of scintillator used. In particular it is useful to introduce a term for the transfer efficiency of the optical photons R_S, a term for inhomogeneity R_i and a term for nonproportionality R_n

$$R_S^2 = R_t^2 + R_i^2 + R_n^2 \tag{2.16}$$

The interest lies in the fact that the two terms, for inhomogeneity and nonproportionality, account for the intrinsic resolution of the crystal. Inhomogeneity arise from possible imperfections of the scintillator, such as local variations in the concentration

of the dopant or optical defects. Non proportionality arise when scintillators show deviation from stability of excitation spectrum, that is when linearity between energy of the excitation and relative light output is not preserved. This is particularly important for low energy excitation, since scintillation phenomena occur mainly on the surface. Non proportionality is a cause of the statistical nature of the creation of secondary electrons and photons and contribute to worsen the resolution.

2.4.4 Cerenkov effect

The effect of Cerenkov radiation brings important information both in high energy physics and time resolved PET. Cerenkov radiation occurs when a charged particle passes through a dieletric medium at a speed greater than the phase velocity of light in that medium. The phase velocity of light in a medium of refractive index $n > 1$ is

$$v_{light} = \frac{c}{n} \tag{2.17}$$

A charged particle can travel faster than the speed of light if, given its velocity v_p

$$\frac{c}{n} < v_p < c \tag{2.18}$$

This translates to the following condition for the β coefficient of the particle

$$\beta = \frac{v}{c} > \frac{1}{n} \tag{2.19}$$

For a particle of a given mass thus the energy threshold is

$$K_t hr = mc^2 \left(\frac{\sqrt{n^2 - 1}}{n} - 1 \right) \tag{2.20}$$

The phenomenology of Cerenkov effect can be explained considering the polarization of the medium caused by a charged particle trasversing it. Below the Cerenkov threshold the dipoles sorrounding are simmetrically arranged around the path. As

the particle crosses the threshold it travels faster the the speed at which it interacts with the dipoles. This simmetry breaking leads to a non-vanishing dipole moment and thus to the formation of a wave front.

Cerenkov photons are emitted at a characteristic angle in the forward direction, obtained via simple geometrical considerations. The distance traveled by the charged particle in a time t is $t \cdot \beta \cdot c$ whereas the distance along which the photon propagates is $t \cdot c/n$ as shwn in fig.

Therefore the characteristic angle at which photons are emitted can be calculated as

$$cos(_C) = fractc/nt\beta c = \frac{1}{n\beta} \tag{2.21}$$

As will be shown in the next chapter, the direction of emission retains a primary interest in the field of particle identification, while it has little impact on timing measurement on PET scanners. It is worth to be noted though that the Cerenkov photons are emitted promptly, taking a relevant share of the first incoming photons.

It is useful to consider the number of emitted photons per unit length by a charged particle in function of the wavelength

$$\frac{d^N}{d\lambda dx} = \frac{2\pi z^2 \alpha}{\lambda^2}\left(1 - \frac{1}{\beta^2 n^2(\lambda)}\right) \tag{2.22}$$

Neglecting dispersion in the medium, and integrating over an appropriate interval of waveleghts we obtain that the photons are emitted mostly in the UV range.

$$\frac{dN}{dx} = 2\pi z^2 \alpha \left(1 - \frac{1}{\beta^2 n^2(\lambda)}\right) \int_{\lambda_1}^{\lambda_2} \frac{d\lambda}{lambda^2} = 2\pi z^2 \alpha sin^2\theta_C \left(\frac{1}{\lambda_1} - \frac{1}{\lambda_2}\right) \tag{2.23}$$

2.5 Scintillators in PET detectors

[75mm] Nulla facilisi. In vel sem. Morbi id urna in diam dignissim feugiat. Proin molestie tortor eu velit. Aliquam erat volutpat. Nullam ultrices, diam tempus vulputate egestas, eros pede varius leo. Quoteauthor Lastname

3

Photo detectors

After the scintillation phase in the crystal, visible photons are generated and coupled to a photodetector. At this stage the photodetector generates an eletric signal related to the photon rate, by generating free electrons in vacuum or electron-hole pairs in a semiconductor.

As they are used as fundamental components of the experimental apparatus the vacuum photodetector technology and the solid state technology will be presented. Vacuum photodetectors are characterized by the production of free electrons in an external photocathode by photoelectric interaction. The produced electrons undergo acceleration in a focused electric field and are multiplied by secondary interaction before being transfered to the read out circuitry. Photo multiplier tubes (PMT) and micro channel plates (MCP) are prominent examples of vacuum technology.

In the case of solid state photo detectors, photons interact directly in the bulk material, where electron-hole pairs are produced. The pairs are then accelerated in the electric field and multiplied by ionization in the semiconductor itself. In the work presented here, Silicon photo multipliers (SiPM) are used as representative of this kind of detector.

3.1 Photo multiplier tubes

Photo multiplier tubes are largely used vacuum photo detection devices and have been diffusively discussed in literature. In figure 3.2 the main elements of a photo

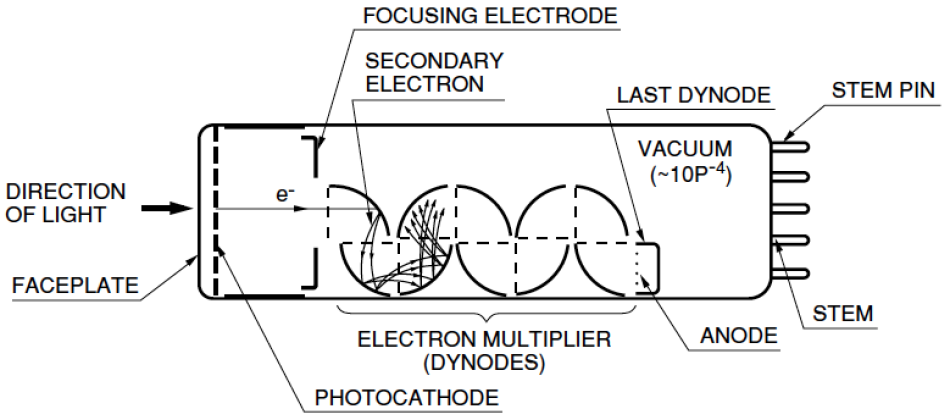

FIGURE 3.1: Longer caption for actual body of dissertation. Figure captions should be BELOW the figure.

multiplier tube are sketched:

- a photocathode, which converts visible photons into an electron flux
- an electron-optical input system which focuses and accelerates the electron flux
- an electron multiplier consisting of a series of secondary emission electrodes (dynodes)
- an anode, which collects the electron flux and supplies the output signal

Photoemission is due to a fraction of the incident visible photons that transfer enough energy to the electrons of the photo cathode to extract them. Then the focusing system allows the freed electrons to reach the first dynode, i.e. the first multiplication stage. The electrons are accelerated and focused by eletric field between the dynodes and the required potential gradient is usually guaranteed by a voltage divider.

3.1.1 Properties of PMT

- quantum efficiency Photocathode are usually made of deposited photo emissive semiconductor. They can be semi transparent or opaque, depending on the place where the emissive material is deposited with respect to the input window. The most used materials are silver-oxygen-caesium ($AgOCs$), antimonyum caesium ($SbCs$), and the bi-and trialkali compounds $SbKCs$, $SbRbCs$, and $SbNa_2KCs$. The most important parameter to be considered is the cathode radiant sensitivity, defined as the ratio of the cathode current I_p to the incident flux Φ

$$S_k(A/W) = \frac{I_p(A)}{\Phi_e(W)} \tag{3.1}$$

The incoming photons have usually a certain spectral composition and the cathode is not uniformly sensitive in this range. With this respect the most used quantity is the quantum efficiency, that is the ratio of the number of photo electrons emitted, n_k, to the number of incident photons, n_i

$$QE = \frac{n_k}{n_i} = S_{k,\lambda}\frac{h\ni}{e} \tag{3.2}$$

where $S_{k,\lambda}$ is the monochromatic sensitivity, defined as

$$S_{k,\lambda} = \lim_{d\lambda\to 0}\frac{dI_p}{d\Phi_e} \tag{3.3}$$

- gain if the number of photo electrons that reach the first dynode is n, and the gain of the dynode is g_1, the number of secondary electrons is $n \cdot g_1$. If g_i is the gain of the single dynodes, after N stage the number of electrons collected at the anode are

$$n_a = n\prod_{i=1}^{N} g_i \tag{3.4}$$

It is possible to define the gain of the photo multiplier as the ratio I_a/I_p where I_a is the anode current given by a photo current I_p. If we define a collection efficiency for each dynode, depending of geometrical parameters, η_i, then the gain G is

$$G = \eta \prod_{i=1}^{N} \delta_i \eta_i = \eta \prod_{i=1}^{N} g_i \tag{3.5}$$

- transit time spread Transit time spread is the transit-time fluctuation of the signal when identical light pulses hit the same part of the ohiti cathode. The time resolution of a tube is then often quoted as the FWHM of the probability distribution of the fluctuations. If the probability distribution of electrons arriving at the andode is assumed to be gaussian, then the response $R_\delta(t)$ to a delta-function light pulse is

$$R_\delta(t) = \frac{1}{\sigma_R \sqrt{2\pi}} exp\left(-\frac{(t - t_{tts})^2}{2\sigma_R^2}\right) \tag{3.6}$$

where t_{tts} is the mean transit time.

3.2 MCP-PMT

A micro channel plate is a two-dimensional array of glass capillaries mounted in parallel as shown in fig The diameter of the channels lies in a range of 5 to 20 microns and their internal walls are treated so to hava a defined electrical resistance and secondary emissive properties. At both ends of the plate high voltage is applied, so that a primary electron impinging on the wall of a channel produces a multiplication chain. Since they resemble in function a structure of dynode, microchannel plates are usually used in combination with vacuum detector technology in an assembly known as MCP-PMT. An MCP-PMT consists of an entry window, a photo cathode one or more micro channel plates and a collecting anode. To operate and MCP it

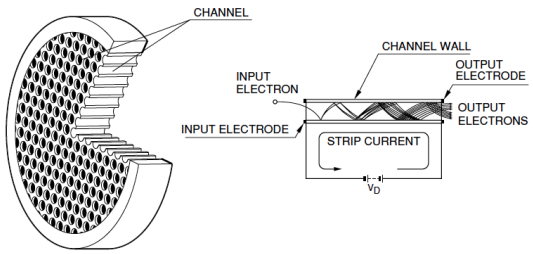

FIGURE 3.2: Longer caption for actual body of dissertation. Figure captions should be BELOW the figure.

is necessary to provide a certain voltage to the system. To this purpose standard voltage divider circuits are usually adopted, in order to guarantee mostly drifting spaces for electrons before and after the photocathode and multiplication in the MCP stack.

3.2.1 Properties of MCP

- quantum efficiency In terms of quantum efficiency they do not differ from standard PMTs, since they make use of the same technology in terms of photo cathodes.

- gain The gain of an MCP-PMT depends primarily on the number of plates stacked. Geometrically is determined by the length-to-diameter ratio af a channel α, as

$$G = exp(\frac{\Delta \cdot L}{d}) = exp(\Delta \cdot \alpha) \tag{3.7}$$

  where *Delta* is the gain factor and depends on the plate material, L and d are, respectivelly, the length and diameter of the micro tube.

- ion feedback and electron backscattering Strongly correlated with the characteristics of gain are the problems of ion-feedback and electron backscattering. As the voltage, and thus the gain, increases, it is more and more likely for a

photoelectron to be backscattered towards the photo cathode or for an ion to undergo the same process from the stack. Ions can be commonly stripped from residual gas in the drifting area or from interaction in the plate. This leads to the production of secondary pulses, that contribute in the worsen of the time response of the device. Connected to this is also the issue of ageing, since ion bombardment damages the photocathode and it is more and more likely as the vacuum in the device degrades with time. Partial solution to this problem has been found by depositing an Aluminum protection layer on the plate and by modifying the inclination of the micro tubes in the so called Chevron geometry**?**.

- time characteristics The rise and fall time of a MCP-PMT are ultra-short, due to the multiplication characteristics of the device. This translated into typical signal contained in a few nanoseconds, or even less. For timing application though the most important parameter to consider is the transit time spread (TTS). The TTS is the spread in the arrival time of a bunch of photon produced by a converted electron in the photocathode. The time response of MCP-PMTs will be analyzed further in the next chapters.

3.3 Silicon photo multipliers

Recently solid state photo detectors have become competitive with vacuum devices, and for some applications they represent the ideal solution. Their advantage lies in the high photon detection efficiency, their low sensitivity to high magnetic fields, their compactness and cost efficiency. In particular the insensitivity to high magnetic fields, given by the feature that no electrons are travelling in the vacuum between dynode and dynode, makes the solid photo detector the first choice for PET-MRI scanners or high energy experiments. With respect to the MCP-PMT, also char-

acterized by high operability in magnetic fields, silicon devices still mantain a high photon detection efficiency, that is the conversion efficiency of incoming photons in to electron hole pairs determining in principe a better energy and time resolution. Solid state photo detectors are usually p-n junctions biased reversely and depending on the value of the bias voltage different operational parameters adapt to fundamentally three modes. As seen in figure the voltage can applied can be low, as in photo diodes, leading to low currents proportional to the incoming flux. Moving towards the proportionality region the freed electrons are able to ionize further, thus determining a net gain of the device. Avalanche photodiodes (APDs) are a common device operated in this region. Finally a third region, characterized by non-proportionality is the precipous operating segment of Geiger mode APD (G-APD). In the Geiger mode region both electrons and holes are able to futher ionize the bulk, and the device is sensible to single photo electrons. The created avalanche must be quenched either externally by a series of quenching resistors or actively. Many G-APD cells connected in parallel are the basic structure of silicon photo-multipliers (SiPM) or multi pixel photon counters (MPPC).

3.3.1 Analog SiPM

The structure of an analog SiPM is composed by series of Geiger mode cells in parallel, and the self sustained avalanche is usually quenched by external resistors or active quenching circuitry. The basic schema of a standard SiPM with quenching resistors is shown in fig.

The structure of a G-APD optimized for detection of blue light is shown in fig. On top of the low resistivity bulk layer an epitaxial layer with a high dopant concetration region is located. The implantation of opposite charge consitutes the p-n junction with a very thin layer extremely doped to assure electric field uniformity. The cell and the quenching resistor are connected on the top surface. Finally a passivation

layer (SiO2) protects the device. Due to its low index of refraction (1.55 in the blue) with respect to the one of Silicon (3.5) Fresnel losses can occurr, usually compensated by the presence of anti-reflection coatings.

3.3.2 Properties of SiPM

- photon detection efficiency the photon detection efficiency can be defined as

$$PDE = QE \cdot \epsilon \cdot P_{avalanche} \tag{3.8}$$

  where QE is the quantum efficiency, ϵ is the geometric fill factor and $P_{avalanche}$ is the probability of triggering an avalanche. The QE has already been introduced for ordinary photo cathodes and it is comprehensive of Fresnel losses. The fill factor ϵ is defined as the ratio of the sensitive area to the total area of the detector. Finally the $P_{avalanche}$ is the probability of an electron or hole to cause an avalanche and it depends on the bias overvoltage.

- gain The gain of an analog SiPM can be written as

$$G = \frac{C \cdot U_{ov}}{q} \tag{3.9}$$

  where C is the cell capacitance, U_{ov} is the bias overvoltage and q is the charge $q = 1.602 \cdot 10^{-19} C$. This value is tipically between 10^5 and 10^7.

- Spurious events

  Dark count is the random production of charge carriers in the depleted region which leads to a regular signal. This type of unwanted event is tipically uncorrelated, provided the the darc count rate (DCR) is low enough. It strongly depends of temperature, and typical values range between $100kHz$ to few MHz at $25C$. Optical crosstalk on the other hand is determined by the trigger of an

avalanche by an optical photon produced in a neighbouring cell. Indeed optical photons produced in avalanches can travel to other cells, causing correlated spurious pulses. These pulses can occur even after a delay of several microseconds, due to the secondary photons generating electron hole pairs. Moreover charge carriers can be trapped in the bulk and released tens to hundreds of nanoseconds later determining afterpulsing.

- saturation

  If SiPMs are exposed to high photon fluxes, saturation effects may occurr. The detector is intrinsically limited by the number of cells: if the number of photons is small compared to the number of cells provided PDE correction, the SiPM signal is proportional to the light signal. In the opposite case, the signal is saturated.

3.3.3 NINO

Signal generated by SiPMs are in the range of Thus we make use of low noise electronics to read out the detector. In the study presented the ultrafast front-end preamplifier-discriminator chip called NINO, developed at CERN**?**. Originally designed for the time-of-flight subdetector of the ALICE experiment, it matches the main requirements of a SiPM readout, that is speed, low noise, minimum slew rate, low input impedance. The chip has eight channels, designed for differential readout. Each channel is is characterized by an amplifier with 1-ns peaking time, a discriminator with a minimum detection threshold of 10 fC and an output stage.

The input stage is a current-to-voltage converter and the subsequent signal amplification is performed with four identical cascade amplifiers that operate as a discriminator as well. The threshold is set by a voltage difference applied on two symmetrical inputs. The NINO chip makes use of the time-over-threshold technique: a squared

output pulse is produced when the leading edge is above the set threshold, encoding the timing information. The width of this signal, on the other hand, is a function of the charge collected, thus encoding the energy information.

[75mm] Nulla facilisi. In vel sem. Morbi id urna in diam dignissim feugiat. Proin molestie tortor eu velit. Aliquam erat volutpat. Nullam ultrices, diam tempus vulputate egestas, eros pede varius leo. Quoteauthor Lastname

4

MonteCarlo simulation tools

4.1 Ray tracing

4.2 Geant4

4.3 SLitrani

4.4 A comparison

[75mm] Nulla facilisi. In vel sem. Morbi id urna in diam dignissim feugiat. Proin molestie tortor eu velit. Aliquam erat volutpat. Nullam ultrices, diam tempus vulputate egestas, eros pede varius leo. Quoteauthor Lastname

5

Role of crystals in fast timing

[75mm] Nulla facilisi. In vel sem. Morbi id urna in diam dignissim feugiat. Proin molestie tortor eu velit. Aliquam erat volutpat. Nullam ultrices, diam tempus vulputate egestas, eros pede varius leo. Quoteauthor Lastname

6

Gamma measurement

6.1 Fisica

The physics behind gamma interaction have been already introduced in chapter... In order to build a time correlated single photon counting experiment two time signals are necessary, a start signal and a stop signal. A simple way to obtain this is to use a β^+ active isotope, such as Na^{22}. This isotope emits a positron according to the decay reaction $^{22}Na \rightarrow^{22} Ne + \beta^+ + \ni_e + \gamma$. The positron yield is relatively high, 90.4%, and competitive processes are electron capture (EC) and direct transition to the Ne ground state. In the positron emission case the Ne ground state is reached after 3.7 ps by emission of a γ quantum of 1.274 MeV. The half life of the isotope is 2.6 years. It is worth to note that, as outlined in chapter

the Cerenkov threshold for heavy scintillators is below the energy of the annihilation gamma produced by the isotope.

6.2 Apparato

The components of the apparatus were placed in a cooled black box. Cooling is necessary to mantain the performance of SiPM

The start signal is obtained by mean of a LSO crystal. The reference crystal is readout by a SiPM board amplified by a NINO chip.

6.3 Preliminaries

6.3.1 Characteristics of the start signal

6.3.2 Characteristics of the stop signal

6.4 Data analysis

6.4.1 IRF measurements

6.4.2 Cuts

6.4.3 Fit procedure

6.4.4 Measurements

[75mm] Nulla facilisi. In vel sem. Morbi id urna in diam dignissim feugiat. Proin molestie tortor eu velit. Aliquam erat volutpat. Nullam ultrices, diam tempus vulputate egestas, eros pede varius leo. Quoteauthor Lastname

7

VUV measurement

7.1 High Harmonic Generation

When an atom is exposed to a strong laser field it can absord a large number of photons through non linear processes. This energy can be transferred back to the photon field. The phenomenon of high order harmonic generation of a laser field is a nonlinear effect that results in the emission of photons of frequency multiple of the source frequency. For example a rare gas traversed by a sufficiently power laser field may give rise to harmonic generation. In fig the main details of the high harmonic generation process are summarized, in a semi-classical configuration and as a quantum wave process. If the laser field is strong enough ($\sim 10^{10}$V/m), it can allow the electron to tunnel through the barrier. The electron itself sits unperturbed in the well until the field of the laser sums to the atom potential bending it. The electron gets accelerated in the laser field and it can recollide with the atom itself. The electron kinetic energy is then transferred into photons. The cut-off energy can be calculated by examining the maximum energy the ionized electron can gain in the

electric field of the laser, that is

$$E_{max} = I_p + 3.17U_p \tag{7.1}$$

where U_p is the ponderomotive energy from the laser and I_p is the ionisation potential. The recollision leads to the emission of a very broad light spectrum. The ionization and recollision happen on each half cycle of the laser pulse, and the spectra are added coherently. As a consequence the spectrum is structured in odd harmonics. High harmonics constitute a source of soft X-rays that retains the time characteristics of the driving laser, in terms of bunch structure and repetition rate. The harmonic cut off varies with the laser intensity up to saturation. The saturation intensity depends on atomic species of the noble gas used as a medium to produce the harmonics.

7.2 Experimental setup

The setup available at CELIA it is presented in **?**. it will be briefly described here. The line is organized in two different room. A first room is devoted to the laser amplification system, while in the experimental room the high harmonics are produced.

7.2.1 Laser beamline

The AURORE beamline is based on a amplified Ti-sapphire femtosecond oscillator. The Ti-sapphire oscillator generates 30 fs pulses, at 1 nJ and a frequency of 80 MHz. Before amplification the pulses are stretched up to 280 ps for optical power reasons. The regenerative pre amplifier brings the energy of the beam to 700 J at 1 kHz. The beam is then amplified in a Ti:sapphire crystal pumped by four synchronised Nd:YLF lasers at 532 nm and 15 W. At the end of the amplification chain the laser beam delivered has a power of 10 W for 170 ps and it is sent to the experimental room.

7.2.2 VUV line

Before high harmonic generation the beam is compressed again down to 35 fs, centered around 800 nm at 1 kHz, with an energy of 4 mJ. A schematic of the HH VUV beamline is presented in fig The elements are under vacuum at a pressure of 10^{-6} mbar. The beam is focused in the fiber containing the gas ($200m$ in diameter and 4 cm length). Depending on the gas used and the pressure condition the energy of the harmonic lines and the efficiency of the process may vary. Tipically in Argon/Neon the energy of the harmonics is between 10 eV and 120 eV. The fundamental beam and the harmonics spread at the exit of the fiber and are sent to the monchromator where a toroidal mirror and a plane grating (470 lines/mm) focuse the selected wavelength on the exit slit. The zero order is suppressed by a plane mirror at an angle tuned on the grating system. The desired VUV-XUV beam selected in energy is then directed to the sample placed in a vacuum chamber. Due to the dispersion by the grating the output pulses are stretched in time, and they have been measured with a VUV-streak camera to be 2-3 ps FWHM.

7.2.3 Detection system

The light produced by the luminescent sample hit by the VUV-XUV radiation is collected by an optical fibre visible-UV of 0.6 mm diameter mounted on a side of the chamber and connected to a monochromator (TRIAX Jobin-Yvon 130) by a focalisation system. The monochromator is equipped with three diffraction gratings, one with 1200 lines/mm and the others with 300 lines/mm. This allows to cover a spectral range between 200 nm and 1000 nm. The emission spectrum is measured by mean of a CCD camera The photon counting device is a Hamamatsu MCP-PMT R3809U-52 model. The DAQ system is shown in fig The signal from the laser trigger is routed into a Ortec Pico Timing Discriminator (model 9307). A first output is directed directly to a Ortec Time to Analog Converter (model 9308). A second

output is directed to a Lecroy Quad Coincidence Unit (model 622). The MCP-PMT signal is preamplified by a ORTEC 1-GHz preamplifier (model 9306) with a gain of 100 and then sent to a second Pico Timing Discriminator. One output is sent to the Lecroy Quad Coincidence Unit and a second one delayed by 60 ns and sent to the TAC. The last unit is required since the laser trigger has a fixed delay. A third output is sent to a SR400 Gated Photon Counter (Stanford Research System) along with the output of the Lecroy coincidence unit. The SR400 Gated Photon Counter allows to determine the rate of counts at the MCP detector, to keep under control the fraction of biased events. The TAC guarantees a 16-bit digital resolution in the range 0-325 s down to a binning of 1.22 ps and its signal is sent to a computer for the software system to finally determine the delay between the MCP and the laser trigger.

7.3 Preliminaries

7.3.1 VUV spectrum

7.3.2 Estimation of the IRF

7.3.3 Control of the bias fraction

7.4 Results

Appendix A

Populo Ornatus

Ut quando convenire scripserit mei, ut accusam noluisse eam. At scripta democritum quo, reque everti an qui, posidonium efficiendi ut mel. Pro an reque habemus, augue nemore conceptam in vim. Eu cibo ancillae takimata usu.

No vis albucius rationibus, eum doming ceteros constituto id. Ad suas zzril laudem cum. Natum mollis singulis vel te, ea elit imperdiet duo, odio inermis et eos. Nam ad vocibus tractatos, sit no vidisse diceret omnesque, mollis omnesque ea mea.

Ut est ridens principes scribentur, menandri interesset adversarium ius ut. Ut duo elit dissentias, at sea eleifend scripserit, eam nibh rebum definitiones an. Cum te quaeque epicuri mentitum, his elitr essent et, in sea habeo aliquid convenire. Quo euismod sadipscing definitionem an, ut duo iusto aliquando, graece appetere ne nec.

Consul imperdiet dignissim vis et, mei liber vidisse principes et, eu nam docendi voluptua democritum. Qui no dicat tamquam sanctus, saepe tincidunt no mel. Pro ignota albucius consetetur in, sint qualisque assueverit eam ut, vis graeco denique signiferumque ne. Sale appellantur contentiones eu his, pro magna ornatus ut, ad vidit omnesque euripidis pri. Sea congue moderatius in, his dicit suscipit no, mei

ei incorrupte assueverit. Nusquam nominavi et quo, idque delenit vim an, posse quaeque an mea.

Suas elitr lucilius sit an, aeterno persius vel eu. Mel at essent aperiam repudiare. Tale consul eum ne, eam no meis delenit iudicabit, an sint mutat pri. Nec no clita propriae pericula, duo explicari gubergren ei. Ne sit autem nominavi, te falli deserunt per. Quo tractatos suscipiantur ex, electram dignissim usu no, cu congue iriure vivendo vim.

At vero graeci fuisset his, quo similique persequeris ad. Ex est graece mandamus, antiopam voluptatum his ea. Assum appellantur mel an, ei mea veri commune efficiendi. Pri blandit urbanitas no. Nam ex enim reque, ut nec iusto regione ullamcorper, facer harum pertinacia mei ei. Erant veniam imperdiet an eam, veniam mucius equidem ius eu, at scripta labitur est.

Et quo soluta graecis accommodare. Tamquam mentitum menandri vim ut. Ut nec melius senserit, ut mei sale aeque. Prompta delectus mea te, fierent adipisci ad per, mei odio pertinax senserit et. Per ut persius singulis. Id qui malorum iracundia, semper conceptam cu sed.

Vis nominavi urbanitas intellegat an, ut numquam deseruisse sea. Et quo dico aeque adipiscing, ius ea commodo epicurei, eum cu nulla imperdiet efficiantur. Ea cum simul scripserit. Ius reque decore voluptaria ei, nec sensibus mediocrem eu, sit iriure vivendo ad. At munere maiestatis mel, ex persius honestatis nec. Nihil omnes definiebas duo cu, dicat ancillae no vix. No est prompta apeirian, mel ad quaestio theophrastus mediocritatem.

Persequeris intellegebat disputationi et nec, nam ne alia solum reque, ad pri clita appellantur reprehendunt. Clita iracundia ex cum, placerat invidunt dissentias ius id. Possit dictas recteque sed ne. At eam singulis recusabo intellegat, ius in probo clita posidonium, id atqui paulo rationibus pro. Ut elit mucius qui. Mel ea ubique nostrud takimata. Cu eos vituperatoribus temporibus feugait.

Per putent nusquam oportere cu, nullam discere te sea, an vix quot mutat. Cibo reque nostrum nec eu, justo mucius aeterno vis id. Facer tempor cu vix, ex saepe similique maiestatis qui, ne pro eripuit offendit. Id mel cetero efficiantur. Cum homero aeterno euismod an, vulputate definitiones ne quo.

Sed exerci incorrupte et, usu mundi molestiae reformidans in, at probo vocibus quo. Ex vel aliquip maluisset. Qui enim error an, molestie incorrupte an ius. Id maiestatis temporibus mei, tantas oporteat ocurreret id pri. Ei nam velit doming utroque.

Suas vituperata mel eu, ex veri omnes duo, an modo molestie ius. At vis moderatius dissentias scripserit, nullam aliquam usu no. Cibo diceret sed an. Sea cu ridens convenire.

Pro prima blandit no. His ut dicit iriure oblique, eos meis urbanitas abhorreant te. Usu cu perpetua principes. Mutat utinam insolens id cum. Quo tale iudicabit conclusionemque ex. Eos id harum accommodare.

Vel legere liberavisse ut, et aeque timeam usu. Vis eu dico sanctus appetere, id vix graecis repudiare, ad persecuti mnesarchum mei. No atqui nemore deseruisse eum. Meliore accumsan accommodare in qui, an tation rationibus has, ea nulla aliquip euismod his.

Utinam ridens cum eu. Duo aliquam omnesque cu, sea elitr appetere ea. Mea no quas discere apeirian, munere hendrerit conceptam duo an, nec ad habeo tritani. Vis exerci volumus no. Omittantur reprehendunt no has. Malis accusata necessitatibus no nam.

No solet assentior ius, an ferri dissentiet pro, vix ad tantas offendit. Pro tollit consequat gloriatur ne, eu vix amet posidonium. Errem utamur veritus vix ea. Sed laboramus omittantur id, ut sonet voluptatum has, cu doctus iriure menandri eos.

Regione iudicabit ei per. Cum ea aliquip voluptatibus. Sit in partem explicari. Ne probo labores placerat mei. Ullum pertinax ea his, per cu persius impedit adipisci.

Fabulas ancillae dignissim ei his, ius no nulla melius suscipiantur, ne vel laudem eripuit gubergren.

Ei qui equidem adolescens. Has ad accusata urbanitas voluptatum, no pri ferri dicit. Ne qui veritus omittam neglegentur, usu et lorem audiam mediocrem. Vim falli dictas labitur cu, dolores laboramus constituto id has, sit ea sint summo utroque.

Mei graecis definiebas eu, ad his brute omittam elaboraret. Ridens laoreet eos ne, diam mnesarchum ne sea. Idque everti ea pro, eruditi probatus patrioque eu has. Cum omnes gubergren ex, cum te noster offendit indoctum. Putant dissentiunt duo ex, dicat etiam cu quo. Duo esse probatus complectitur ex, vitae eripuit nostrum no sed, cum odio veri reformidans ex.

Vide ipsum ei vel, at diam nominavi his. Etiam assueverit nam eu, ut habeo nusquam eleifend mei. Pro eirmod perpetua id, minim urbanitas usu no. Vim elitr nominati definitionem ex. Ex tollit quaerendum has, nonumy inciderint eos ne. Vis posse munere honestatis ut.

Eu ornatus meliore usu, enim aeque possim eu cum. Pri ad everti fabellas, at pro omnium convenire repudiare, ut mel hinc minimum. Eam et puto reque mollis. Sed ad ponderum lobortis, cu pro viris vitae. Est et iriure inimicus, eos eu laoreet feugait voluptatum, agam aliquando voluptatibus pro eu.

Ex tale eirmod nec. Illud conclusionemque ad his. Sit augue error in, eu mea labitur voluptua, labores ullamcorper vis te. No usu enim aperiri facilisi. Ad vis brute soluta fastidii, meis mundi iuvaret his ea. Has eu cibo rebum. Mundi numquam repudiare ei cum, pri dicam tritani recusabo ea, pri id appareat qualisque.

Eu facete perfecto nec, te vel tale choro petentium. Mel in essent quodsi, ocurreret corrumpit in pri. Est in fabulas similique elaboraret, in viderer delenit vim. Eu vel paulo graeco viderer. Et ius elit debet latine, ad vel ferri voluptaria appellantur.

Vis ad docendi albucius, ne nam sale prima comprehensam. Adhuc inani accusam ex vis. Utamur labitur adipisci nec ei. No persius conceptam adversarium pro, ei

dicunt officiis lucilius usu. Te pri petentium vituperata, vis at solum dicit quaeque, minimum delectus singulis ei vim. His te nibh patrioque dignissim, qui ne euismod argumentum. Quo lucilius sensibus cu.

Est ea nihil debitis deseruisse, mea ne malis nostrum. Vel cu doctus euismod disputationi. Eos ut harum habemus, minim verear maiestatis mei ut. Te nam mundi deseruisse sententiae, pri an nibh eros velit. Ne omnium torquatos ius. Sit id congue quaeque intellegebat, homero volutpat dissentiunt ne usu, ei elit vituperata reformidans eum.

Ut sed corpora accumsan, his cu vero iriure probatus. Ubique latine ea per, usu no erant facilisis. Augue diceret eruditi ea vel, in diam maiorum ullamcorper eum. Vel no iriure latine suscipiantur, cu nec omittam liberavisse disputationi.

Congue repudiandae delicatissimi ut duo, fastidii iudicabit ut sea, eum integre sadipscing an. Cu vel alii liber, ceteros nostrum expetendis per eu, ne congue gloriatur vulputate cum. Eius fierent pericula has cu. Ea has atqui perfecto. Pericula torquatos ius ei, convenire theophrastus id sea, in dicit facilis facilisis mel. Nam modo diam ocurreret an.

Ferri sensibus eloquentiam quo et, mel an nullam vituperata, mollis dignissim sententiae sit ne. An pro perpetua democritum, te eam feugiat delicata deterruisset. Per minim choro ad, prodesset voluptatum ea usu, ea tempor putent quo. Mazim facete scribentur ea sea. Ea pri doctus feugait, ius eu vituperatoribus menandri, dico munere ubique ne his.

Mel no assum nusquam intellegebat, ius platonem consulatu an. Populo ornatus in sea. Sea soleat salutatus ne. Quo error saepe adolescens at, id cum duis voluptatum. Per maiorum mentitum te. Quem iudicabit percipitur per ea. Qui aliquid eruditi ad, ne vix veritus scripserit.

An duo postea aliquip. Nusquam luptatum id vis. Vim no magna inani. Eos et agam aliquid ancillae, verear ponderum no qui.

Bibliography

Biography

Your biography is limited to one page and must contain

1. Full name
2. Date and place of birth
3. Every degree you've earned, including this one, and where you earned it from.

Mostly, that information is to narrow down which John Smith wrote that dissertation on the mating habits of sea cucumbers. Sexy!

You may also include

1. Any awards you've won related to your discipline since your undergraduate degree.
2. Any fellowships you've held
3. Anything you've published (papers, books, book chapters). Don't be afraid to cite it here, so that the full bibliographic record of your article appears in the bibliography!
4. Where your next job will be, if you know